

## Hydrophobic pockets built in polymer micelles to enhance reactivity of Cu<sup>2+</sup> ions

Zichao Wei,<sup>a</sup> Chung-Hao Liu,<sup>b</sup> Qiang Luo,<sup>a</sup> Srinivas Thanneeru,<sup>a</sup> Alfredo M. Angeles-Boza,<sup>a</sup> Mu-Ping Nieh,<sup>b,c</sup> and Jie He<sup>a,b,\*</sup>

<sup>a</sup> Department of Chemistry, <sup>b</sup> Polymer Program, Institute of Materials Science, and <sup>c</sup> Department of Chemical and Biomolecular Engineering, University of Connecticut, Storrs, CT 06269, United State

Emails: [jie.he@uconn.edu](mailto:jie.he@uconn.edu) (JH)

### 1. Materials

Styrene (99%) and *N,N*-dimethyl acrylamide (DMA, 99%) was passed through a basic aluminum oxide column to remove the inhibitor prior to use. 2,2'-Azobis(isobutyronitrile) (AIBN, 98%) was recrystallized twice from ethanol. 2-pyridinecarboxaldehyde, dimethylformamide (DMF), tetrahydrofuran (THF) ethanol amine, and Cu(NO<sub>3</sub>)<sub>2</sub>·3H<sub>2</sub>O were purchased from Sigma Aldrich and used as received. sodium triacetoxyborohydride (NaBH(OAc)<sub>3</sub>) and dicyclohexyl carbodiimide (DCC). Deionized water with a resistivity of > 10.0 MΩ was double distilled on a water purification system (High-Q Inc. 103S Stills).

### 2. Synthesis of chain transfer agent and polymers

#### 2.1 Synthesis of 2-(bis(pyrid-2-ylmethyl)-*N*-(2-hydroxyethyl)-amino) ethyl benzylsulfinyl thiocarbonyl sulfanyl-propionic acid (DPA-BCTPA)

3-Benzylsulfinyl thiocarbonyl sulfanyl-propionic acid (BCTPA) was synthesized using a method reported previously with minor modification.<sup>1</sup> DPA-containing chain transfer agent (DPA-BCTPA) was synthesized through a coupling reaction between *N,N*-bis(2-pyridylmethyl)-*N*-(2-hydroxyethyl)amine (DPA-OH) and BCTPA.<sup>2</sup> In a typical synthesis of DPA-OH, 4.4 mL (46.7 mmol) of 2-pyridinecarboxaldehyde was dissolved in 70 mL of DCM containing 1.4 mL (23.3 mmol) of ethanolamine. 14 g (66.1 mmol) of NaBH(OAc)<sub>3</sub> was added slowly to the above mixture in 30 min and the mixture was then stirred overnight. The reaction was quenched by adding 80 mL of the saturated sodium bicarbonate aqueous solution. The mixture was separated into two phases, and the DCM phase was collected by using a separation funnel. The aqueous phase was further extracted with 40 mL of DCM twice. The combined DCM solution was then dried with anhydrous Na<sub>2</sub>SO<sub>4</sub> for 4 h. After removal of DCM with a rotary evaporator under vacuum, 4.5 g of yellow oily product was obtained and directly used for the further reaction. <sup>1</sup>H NMR (400 MHz, CDCl<sub>3</sub>): δ 2.86 (t, 2H, S-CH<sub>2</sub>-CH<sub>2</sub>), 3.66 (t, 2H, S-CH<sub>2</sub>-CH<sub>2</sub>), 3.93 (s, 4H, CH<sub>2</sub>-N), 7.12 (m, 2H, H-Py), 7.30 (d, 2H, H-Py), 7.57 (td, 2H, H-Py), 8.51 (d, 2H, H-Py).

Then, DPA-OH (1 g, 4.1 mmol), BCTPA (1.3 g, 4.9 mmol), and 4-dimethylaminopyridine (DMAP) (50.2 mg, 0.41 mmol) were dissolved in 100 mL of DCM. DCC (1.0 g, 4.9 mmol) dissolved in 10 mL of DCM was added dropwise to the reaction mixture under nitrogen (N<sub>2</sub>) at an ice bath in 40 min. The reaction was transferred to room temperature then stirred for 48 h. Afterward, the solid precipitate was filtered. The filtrate was extracted with saturated sodium bicarbonate three times. The crude product was purified using column chromatography (silica, ethyl acetate). 1.2 g of DPA-BCTPA as a yellow oily liquid was obtained. <sup>1</sup>H NMR (400 MHz, CDCl<sub>3</sub>): δ 2.74 ppm (t, 2H, CH<sub>2</sub>-O), 2.88 ppm (t, 2H, CH<sub>2</sub>-S), 3.60 ppm (t, 2H, CH<sub>2</sub>-N), 3.88 ppm (s, 4H, CH<sub>2</sub>-Py), 4.21 ppm (t, 2H, CH<sub>2</sub>-N), 4.62 ppm (s, 2H, CH<sub>2</sub>-S), 7.14 ppm (t, 2H, H-Py), 7.26 ppm (5H, H-Ph), 7.50 ppm (d, 2H, H-Py), 7.63 ppm (td, 2H, H-Py), 8.51 (d, 2H, H-Py).

#### 2.2 Synthesis of macro-RAFT CTA agent of poly(*N,N*-Dimethylacrylamide) (PDMA-DPA) and polystyrene (PS-DPA)

The macro-RAFT agents of PDMA-DPA and PS-DPA were synthesized via RAFT polymerization. Using PDMA-DPA as an example, *N,N*-Dimethylacrylamide (DMA) (4 g, 40.4 mmol), DPA-BCTPA (401.6 mg, 0.81 mmol), AIBN (26.5 mg, 0.16 mmol), were dissolved in 8 mL of anisole. The resulting solution was degassed and purged with N<sub>2</sub> for 20 min. The polymerization was carried out in a preheated oil bath at 70 °C for 12 h. After the reaction, excess DCM was added to quench the polymerization. The reaction mixture was then precipitated in hexane three times then dried under vacuum at 40 °C overnight. The repeat unit number was determined to be 52 using the pyridinyl proton of the DPA end group at 8.5 ppm (2H) as the internal standard in <sup>1</sup>H NMR. Using the similar steps, PS-DPA was synthesized using styrene as the monomer and the reaction was carried out under 80 °C for 12 h. The number of repeat units determined to be 76. The number averaged molecular weight and dispersity of PDMA-DPA and PS-DPA were 6.2 and 6.9 kg mol<sup>-1</sup>, respectively. And the poly dispersity (*D*) is 1.2 and 1.3, respectively, as measured by GPC calibrated by PS standards.

#### 2.3 Synthesis of linear block copolymers (LBCPs)

The linear BCPs of PDMA-*b*-PS-DPA and PS-*b*-PDMA-DPA were synthesized through RAFT copolymerization. Using PDMA<sub>52</sub>-*b*-PS<sub>53</sub> as an example, PDMA<sub>52</sub>-DPA (1.36 g, 0.24 mmol) as the macro-CTA, St (2 g, 19.2 mmol) and AIBN (7.9 mg, 0.048 mmol) were dissolved in the 0.8 mL anisole. The solution was degassed and purged with N<sub>2</sub> for 20 min. The polymerization was conducted in a preheated oil bath at 80 °C for 7 h. After polymerization, excess THF was added to the reaction mixture to stop the reaction. The reaction mixture was then precipitated in hexane three times. The samples were dried under vacuum at 40 °C overnight. The repeat unit number of PS was determined using <sup>1</sup>H NMR. The broad peak at ~2.8-3.2 ppm (6H) of PDMA was used as an internal standard to compare with the aromatic protons of PS at 7.0-8.0 ppm. The *M<sub>n</sub>* and *D* of PDMA-*b*-PS were measured by GPC calibrated by PS standards. The characterization results for all the BCPs were summarized in Table 1. The BCPs of PS-*b*-PDMA-DPA were synthesized using PS-DPA to be the RAFT agent and DMA to be the hydrophilic monomer.

## 2.4. Preparation of Cu<sup>2+</sup>-containing micelles

Cu<sup>2+</sup>-containing polymer micelles were prepared in methanol, which is a non-solvent of PS but a good solvent of PDMA. For example, 40 mg of P3 was firstly mixed with 4 mL of methanol and the resulting solution changed the bluish color. Then the solution was transferred into a preheated oil bath at 100 °C to reflux until the solution changed clear (~10 minutes). Cu(NO<sub>3</sub>)<sub>2</sub> solution was added to the solution with the same equivalence of DPA then heated for another 30 mins. The solution temperature was gradually cooled down to the room temperature.

## 2.5. NMR experiments

5 mg of BCPs, such as P3 and P6, dissolve into 600 μL *d*<sub>6</sub>-acetone <sup>1</sup>H NMR spectra were recorded on a Bruker Avance 400 MHz spectrometer. The same equivalence of Zn(NO<sub>3</sub>)<sub>2</sub> of DPA was added to polymer solution and <sup>1</sup>H NMR spectra were collected to monitor the chemical shift of DPA. With the addition of D<sub>2</sub>O at different ratios, <sup>1</sup>H NMR spectra were collected to confirm the location of the ligand during micellization.

## 2.6. Titration with Cu(NO<sub>3</sub>)<sub>3</sub>

The titration of PS-DPA was performed against Cu(NO<sub>3</sub>)<sub>3</sub> solution in DMF and monitored by UV-vis spectroscopy. In a typical experiment, 5 mg of PS-DPA dissolved into 800 μL DMF placed in a 1-mL quartz UV crevette. Then 20 μL of 0.02 mM Cu(NO<sub>3</sub>)<sub>2</sub> DMF solution was added to the polymer solution each time to determine the absorbance at 650 nm. The absorbance was measured until the saturation point was reached. A plot of absorption at 650 nm vs equivalents of Cu<sup>2+</sup> ions corresponding to the number of DPA ligands from polymer is used to find out the molar ratio of Cu<sup>2+</sup> to the DPA ligands.

## 2.7. Kinetics studies

### The kinetics of PNPP hydrolysis

*p*-nitrophenyl picolinate (PNPP) ester hydrolysis reaction was carried out at a constant temperature of 25 °C. The kinetics of PNPP hydrolysis was recorded using UV-vis spectroscopy. Firstly, a solution PNPP was prepared in acetonitrile with the concentration of 1 mg mL<sup>-1</sup>. Then 3 mL PBS buffer (pH = 7) with Cu<sup>2+</sup> containing micelle was added in a quartz cell. 20 μL of PNPP was injected and mixed thoroughly. The kinetics was monitored the absorbance increase at ~400 nm, which is corresponding to one of the products of 4-nitrophenol.

### Arrhenius Plot

The activation energy for PNPP hydrolysis reaction catalyzed by the copper containing micelle was determined from Arrhenius plots. The typical experiment was carried out under different temperatures including 15 °C, 25 °C, and 35 °C. All the kinetics measurements followed up the same procedures and the rate constant was fitted with the first order reaction. To fit Arrhenius plots, the Arrhenius plot (see below) of *lnk* vs. *1/T* was used as,

$$\ln k = -\frac{E_a}{RT} + \ln A$$

where *k* is the rate constant; *E<sub>a</sub>* is activation energy for the reaction; *R* is the gas constant; *T* is absolute temperature (K); and *A* is the pre-exponential factor. The plot was built up by the *lnk* vs. *1/T*. With the linear relationship fitting, the slope can be used to calculate *E<sub>a</sub>* by multiplying with *R*.

### Michaelis-Menten Plot

Michaelis–Menten kinetics experiments were performed by measuring the initial rate (the first 2 min) with different concentration of PNPP. The kinetics measurements were carried out under the same conditions described in the kinetics section except for the substrate concentration. The PNPP concentration varied from 14 to 123 μM. The dependence of the initial rate on the concentration of PNPP was plotted. The fitting was followed up the Michaelis-Menten kinetics models:

$$v = \frac{d[P]}{dt} = v_{max} \frac{[S]}{K_M + [S]}$$

From the plots, maximum velocity (*V<sub>max</sub>*), the Michaelis binding constant (*K<sub>M</sub>*) can be obtained using non-linear regression.

## 3. Characterizations

<sup>1</sup>H NMR spectra were recorded on a Bruker Avance 400 MHz spectrometer. GPC measurements were proceeded with Waters GPC-2 (Waters 515 HPLC pump & Waters 717 Autoinjector) equipped with Waters 2414 Refractive Index Detector (RI). Dimethylacetamide (DMAC) was used as a stationary solvent and the PS as standard for calibration of the molecular weight and dispersity. Transmission electron microscope (TEM) images were carried out by FEI Tecnai 12 G2 Spirit BIO TWIN with an accelerating voltage of 120 kV. The TEM samples were prepared by casting the assembly's suspension on a carbon coated copper grid (300 mesh). The UV-vis spectra of kinetics experiment were recorded by a Cary 60 UV-Vis spectrophotometer: The suspension was placed in a quartz cuvette with a cell path length of 5 mm. SAXS experiments were conducted by using the 16ID-LiX Beamline at the National Synchrotron Light Source II where is located at the Brookhaven National Laboratory (Upton, NY). The concentration of the samples is 1 mg/mL. The solution was loaded in a sample cell sandwiched by two mica windows with a gap of ~2 mm and a window area of 18 mm<sup>2</sup> to allow the beam passing through. The X-ray energy was 13.5 keV. The scattered intensity is expressed as a function of scattering

vector,  $q$  defined as  $\frac{4\pi}{\lambda} \sin \frac{\theta}{2}$ , where  $\theta$  is the scattering angle and  $\lambda$  is the wavelength, yielding a  $q$  range between 0.005 and 2.5  $\text{\AA}^{-1}$ . Radial average and  $q$ -conversion of data were performed by using Jupyter Notebook.<sup>3</sup> The background and transmission correction were conducted via minimizing the intensity of the signal of water peak at  $\sim 2.0 \text{\AA}^{-1}$ . The scattering intensity of the samples was compared against that of the standard (water, which has a theoretical value of  $1.65 \times 10^{-2} \text{ cm}^{-1}$  at 293 K) and rescaled to obtain the absolute intensity.<sup>4</sup>

#### 4. SAXS model

##### **Core-shell spherical model:**

The intensity  $I(q)$  for the core-shell spherical is given by:

$$I(q) = \frac{scale}{V} \times F(q)^2 + background,$$

where

$$F(q) = \frac{3}{V_s} \left[ V_c(\rho_c - \rho_s) \frac{\sin(qR_c) - qR_c \cos(qR_c)}{(qR_c)^3} + V_s(\rho_s - \rho_{solv}) \frac{\sin(qR_s) - qR_s \cos(qR_s)}{(qR_s)^3} \right],$$

where  $V_s$  and  $V_c$  are the volume of the whole particle and core, respectively.  $R_s$  and  $R_c$  are the radius of particles (radius plus thickness) and core radius, respectively.  $\rho_c$ ,  $\rho_s$ ,  $\rho_{solv}$  are the scattering length density of the core, the shell and the solvent, respectively.<sup>5</sup>

##### **Spherical model:**

The intensity  $I(q)$  for the spherical model is given by:

$$I(q) = \frac{scale}{V} \times F(q)^2 + background,$$

where

$$F(q) = \left[ 3V(\rho - \rho_s) \frac{\sin(qr) - qrsin(qr)}{(qr)^3} \right],$$

where the  $V$  is the volume of whole particle.  $r$  is the radius of sphere.  $\rho$  and  $\rho_s$  are the scattering length density of particle and solvent, respectively.<sup>5</sup>

##### **Hayter-Penfold mean spherical approximation (H-PMSA)**

The interparticle interaction can be described by Hayter and Penfold which accounts for the Coulombic interaction among charged particles.<sup>6-7</sup> The  $S(q)$  can be related to the approximated potential,  $U(r)$ . The repulsive potential between two identical spherical macroions of diameter  $\sigma$  is

$$U(r) = \pi \epsilon_0 \epsilon \sigma^2 \Psi_0^2 \exp[-\kappa(r - \sigma)] / r$$

where  $r$  is the interionic center to center distance,  $\epsilon$  is the dielectric constant of the solvent,  $\epsilon_0$  is the permittivity of free space.  $1/\kappa$  is the Debye-Hückle length.  $\Psi_0$  is surface potential which is related to the electronic charge  $z_m$  on the macroion to an approximation by

$$\Psi_0 = \frac{z_m}{\pi \epsilon \epsilon_0 \sigma (2 + \kappa \sigma)}$$

##### **Gaussian chain model**

The form factor can be expressed as

$$P(q) = \frac{2}{q^4 R_g^4} [\exp(-q^2 R_g^2) + (q R_g)^2 - 1]$$

Where  $R_g$  is radius of gyration.

##### **Polymer excluded volume model**<sup>8-9</sup>

The form factor of this model can be described as

$$P(q) = \frac{1}{v U^{1/2v}} \gamma\left(\frac{1}{2v}, U\right) - \frac{1}{v U^{1/v}} \gamma\left(\frac{1}{v}, U\right)$$

Where  $v$  is the excluded volume parameter and  $\gamma(x, U)$  is the incomplete gamma function

$$\gamma(x, U) = \int_0^U dt \exp(-t) t^{x-1}$$

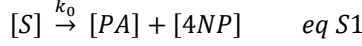
and the variable  $U$  is given in terms of the scattering vector  $q$  as

$$U = \frac{q^2 R_g^2 (2\nu + 1)(2\nu + 2)}{6}$$

## 5. Reverse saturation kinetics

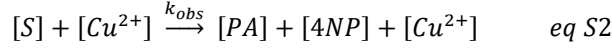
The reverse saturation kinetics fitting is derived from the following equations.

The non-catalytic chemical reaction was considered with a rate constant  $k_0$ :



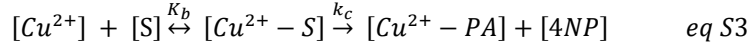
where  $k_0$  ( $\text{min}^{-1}$ ) is the non-catalytic rate constant and the substrate can decompose to picolinic acid (PA) and 4-nitrophenol (4NP);

When the reaction is catalyzed by  $\text{Cu}^{2+}$ -containing micelles, the reaction is:



where  $k_{obs}$  is the obvious rate constant and it is measured from experiments based on first-order kinetics.

In a catalytic process, the catalyst binds with substrate first to form catalyst-substrate complex of  $[\text{Cu}^{2+}\text{-S}]$ , then the formed product of catalyst bound picolinic acid (PA) complexes ( $\text{Cu}^{2+}\text{-PA}$ ) and 4-nitrophenol (4NP):



where  $k_c$  is the catalytic rate constant of bound substrates per  $\text{Cu}^{2+}$  per minute;  $K_b$  is the bonding constant between the substrate and  $\text{Cu}^{2+}$ -containing polymer micelles.

Based on eq S2, the bonding constant of  $K_b$  can be described by:

$$K_b = \frac{[\text{Cu}^{2+}\text{-S}]}{[\text{Cu}^{2+}][S]} \quad eq\ S4$$

The total substrate concentration is:

$$[S]_T = [\text{Cu}^{2+}\text{-S}] + [S] \quad eq\ S5$$

where  $[S]_T$  is the total concentration;

The formation rate ( $r$ ) of 4NP is,

$$r = k_{obs}[S]_T = k_c[\text{Cu}^{2+}\text{-S}] + k_0[S]$$

$[S]_T$  can be substituted by eq S5;

$$k_{obs}([S] + [\text{Cu}^{2+}\text{-S}]) = k_c[\text{Cu}^{2+}\text{-S}] + k_0[S]$$

$$k_{obs}[S] = (k_c - k_{obs})[\text{Cu}^{2+}\text{-S}] + k_0[S]$$

After rearranging the equation by dividing  $[S]$ ,

$$k_{obs} = (k_c - k_{obs}) \frac{[\text{Cu}^{2+}\text{-S}]}{[S]} + k_0$$

$$k_{obs} = (k_c - k_{obs}) K_b [\text{Cu}^{2+}] + k_0$$

$$k_{obs}(1 + K_b [\text{Cu}^{2+}]) = k_c K_b [\text{Cu}^{2+}] + k_0$$

$$k_{obs} = \frac{k_c K_b [\text{Cu}^{2+}] + k_0}{1 + K_b [\text{Cu}^{2+}]}$$

$$k_{obs} - k_0 = \frac{(k_c - k_0) K_b [\text{Cu}^{2+}]}{1 + K_b [\text{Cu}^{2+}]} \quad eq\ S6$$

The linear reaction kinetics can be determined as the reciprocal of  $(k_{obs} - k_0)$  equation of eq S6,

$$\frac{1}{k_{obs} - k_0} = \frac{1}{k_c - k_0} + \frac{1}{(k_c - k_0) K_b} \times \frac{1}{[\text{Cu}^{2+}]}$$

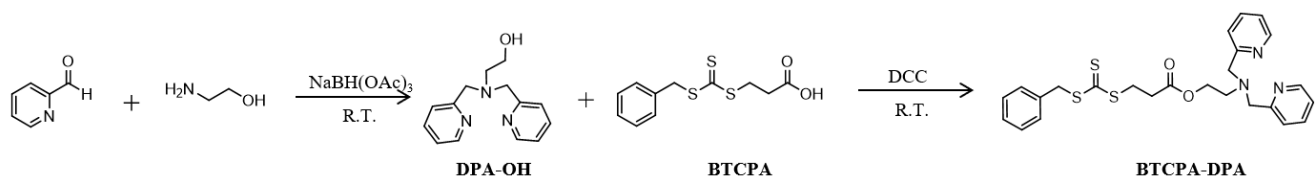


**Figure S1.** Chemical structures to show the synthetic route of DPA-OH and RAFT agent of BTCPA-DPA.

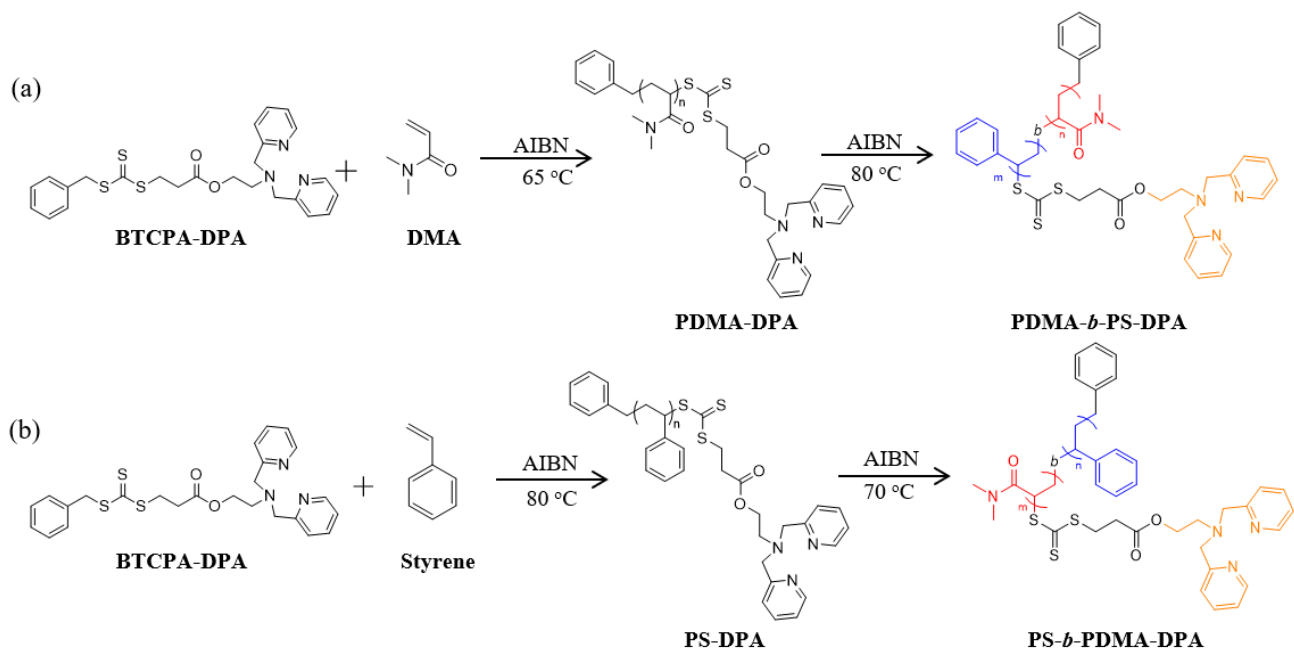


**Figure S2.** (a) Chemical structures to show the synthesis of macro-RAFT agent of PDMA-DPA and the BCPs of PDMA-*b*-PS-DPA; (b) the synthesis of macro-RAFT agent of PS-DPA and the BCPs of PS-*b*-PDMA-DPA

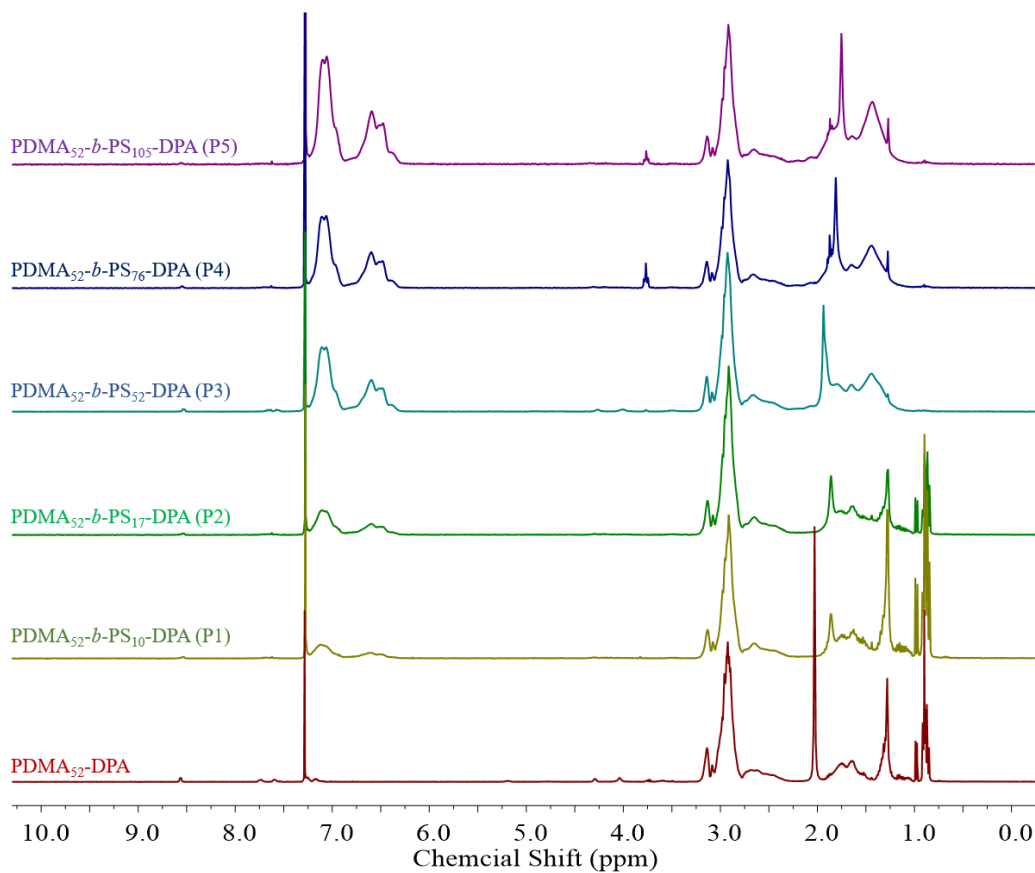


**Figure S3.**  $^1\text{H}$  NMR spectra of copolymers of PDMA-DPA and the BCPs of P1-P5 a measured in  $\text{CDCl}_3$ .

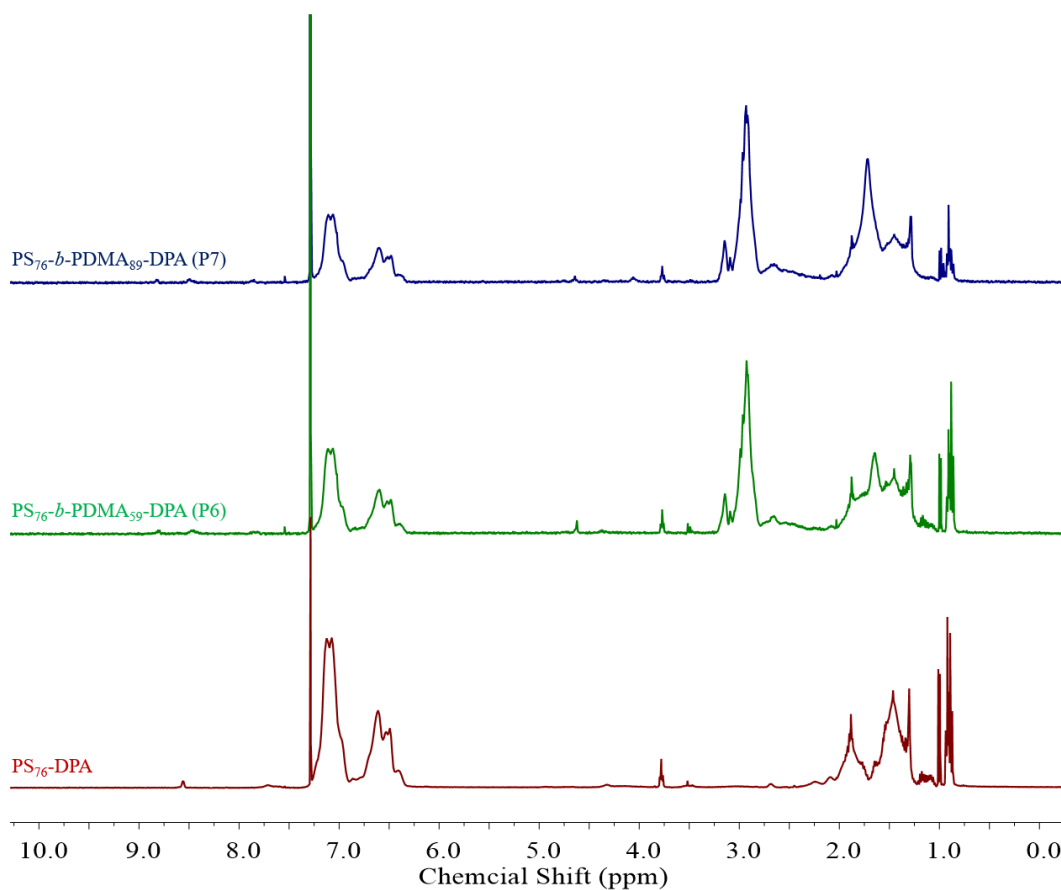


**Figure S4.**  $^1\text{H}$  NMR spectra of homopolymer of PS-DPA (bottom, red), and BCPs of P6 (middle, green) and P7 (top, purple), measured in  $\text{CDCl}_3$ .

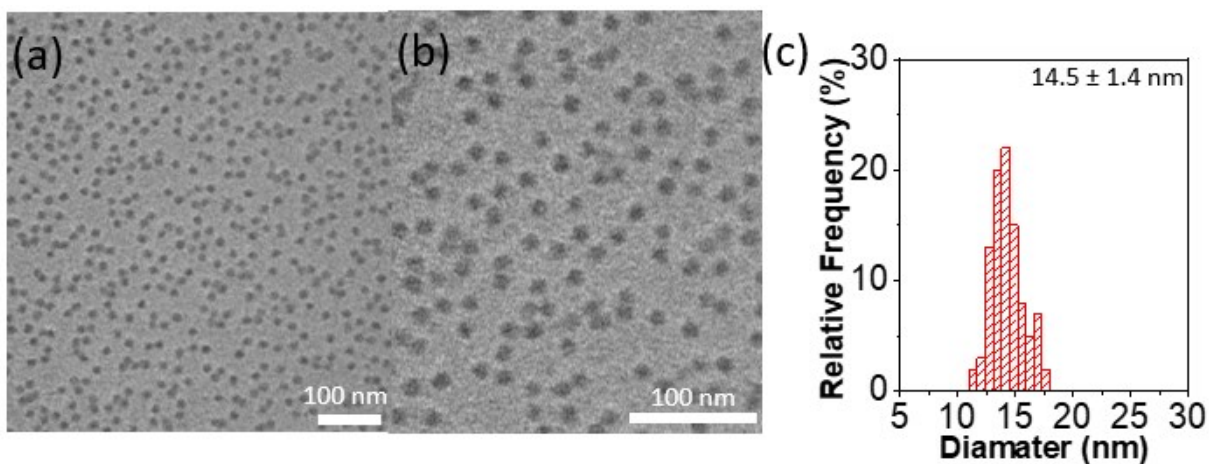


**Figure S5.** (a)-(b) Representative TEM images and (c) the histogram of the average diameter of  $\text{Cu}^{2+}$ -containing micelles of P7.

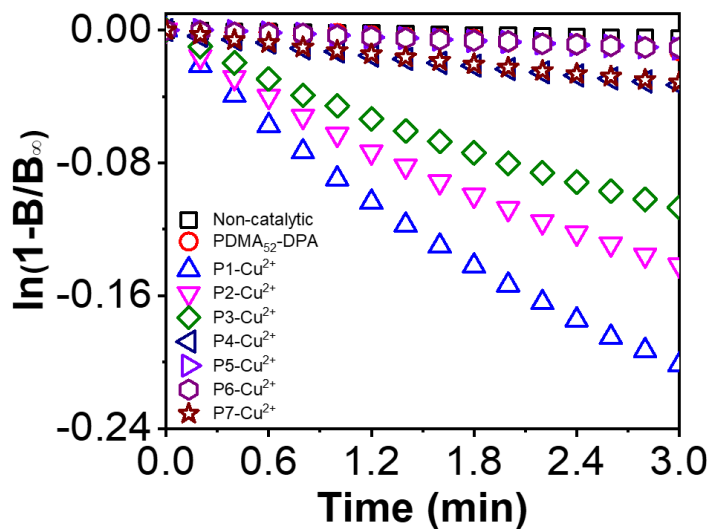


**Figure S6.** First-order reaction kinetics for PNPP hydrolysis of non-catalytic reaction, the reactions catalyzed by  $\text{PDMA}_{52}$ -DPA- $\text{Cu}^{2+}$  and  $\text{Cu}^{2+}$  containing micelles of P1-P7. Reaction conditions:  $[\text{PNPP}] = 27 \mu\text{M}$ ;  $[\text{Cu}] = 2.7 \mu\text{M}$ ;  $T = 25 \text{ }^\circ\text{C}$ . PBS buffer with  $\text{pH} = 7.0$ .

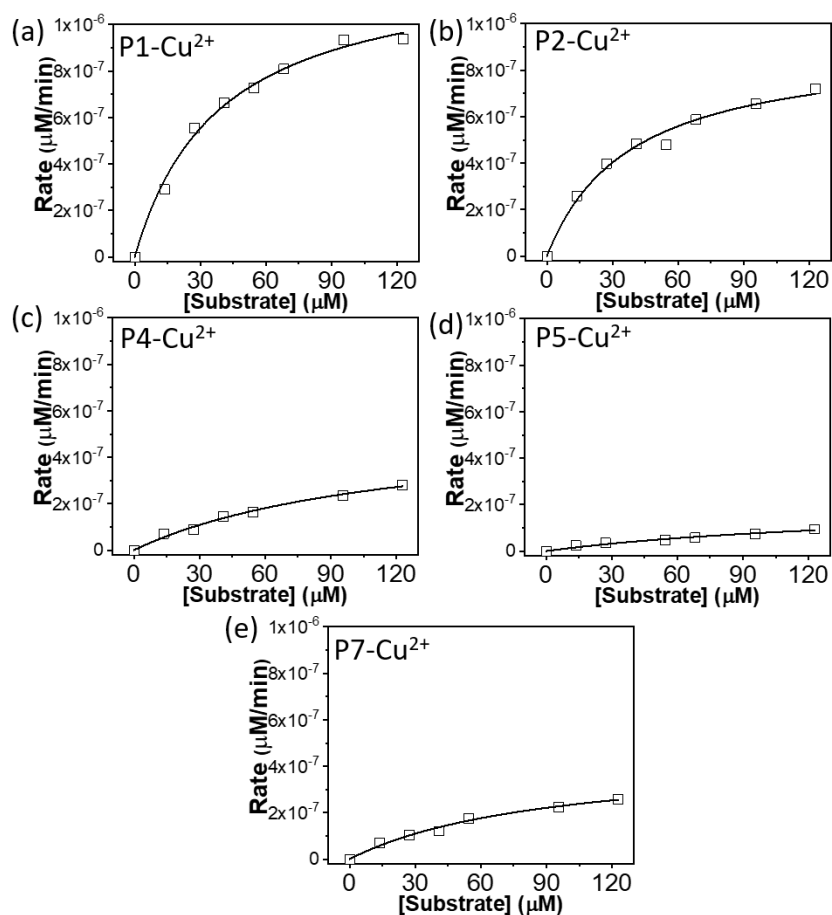


**Figure S7.** Michaelis–Menten plots of PNPP hydrolysis catalyzed by (a) P1-Cu<sup>2+</sup> (b) P2-Cu<sup>2+</sup> (c) P4-Cu<sup>2+</sup> (d) P5-Cu<sup>2+</sup> and (e) P7-Cu<sup>2+</sup> respectively. Reaction conditions: [Cu] = 2.7  $\mu\text{M}$ ; T = 25 °C; [PNPP] concentration was varied from 13.5  $\mu\text{M}$  to 123  $\mu\text{M}$ . PBS bufeer pH = 7.0.

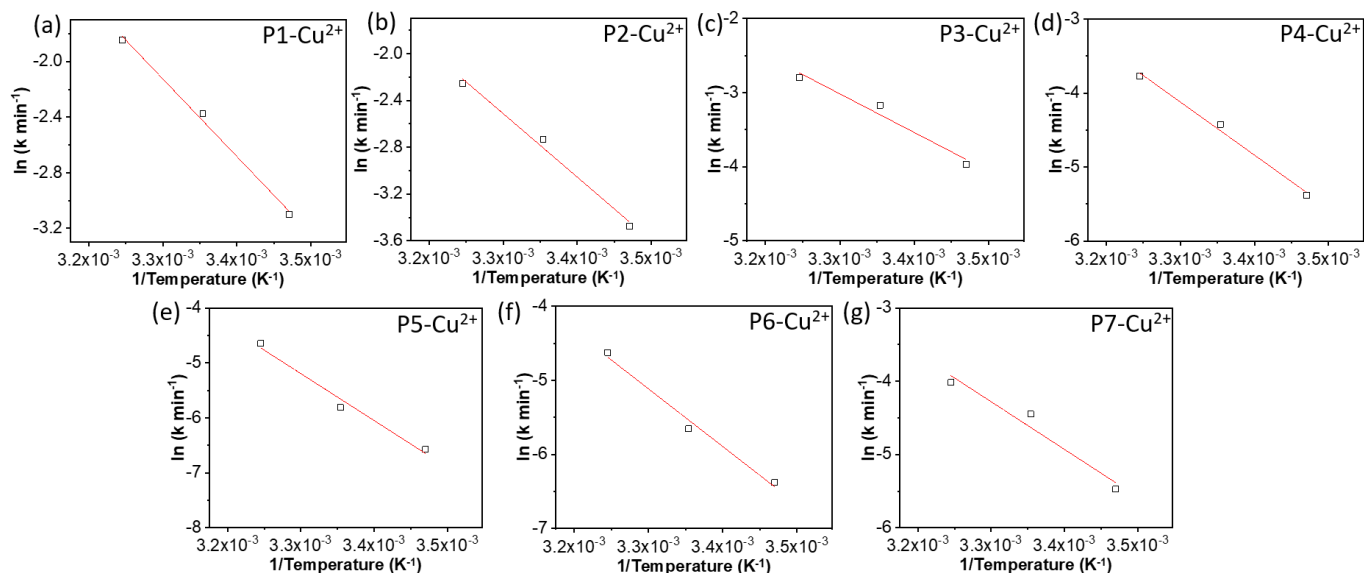


**Figure S8.** Arrhenius plots of PNPP hydrolysis catalyzed by (a-g) P1-Cu<sup>2+</sup>-P7-Cu<sup>2+</sup> respectively. Reaction conditions: [PNPP] = 27  $\mu\text{M}$ ; [Cu] = 2.7  $\mu\text{M}$ ; T = 288 K, 298 K, and 309 K; [Cu] = 2.7  $\mu\text{M}$ ; T = 25 °C; PBS bufeer pH = 7.0.

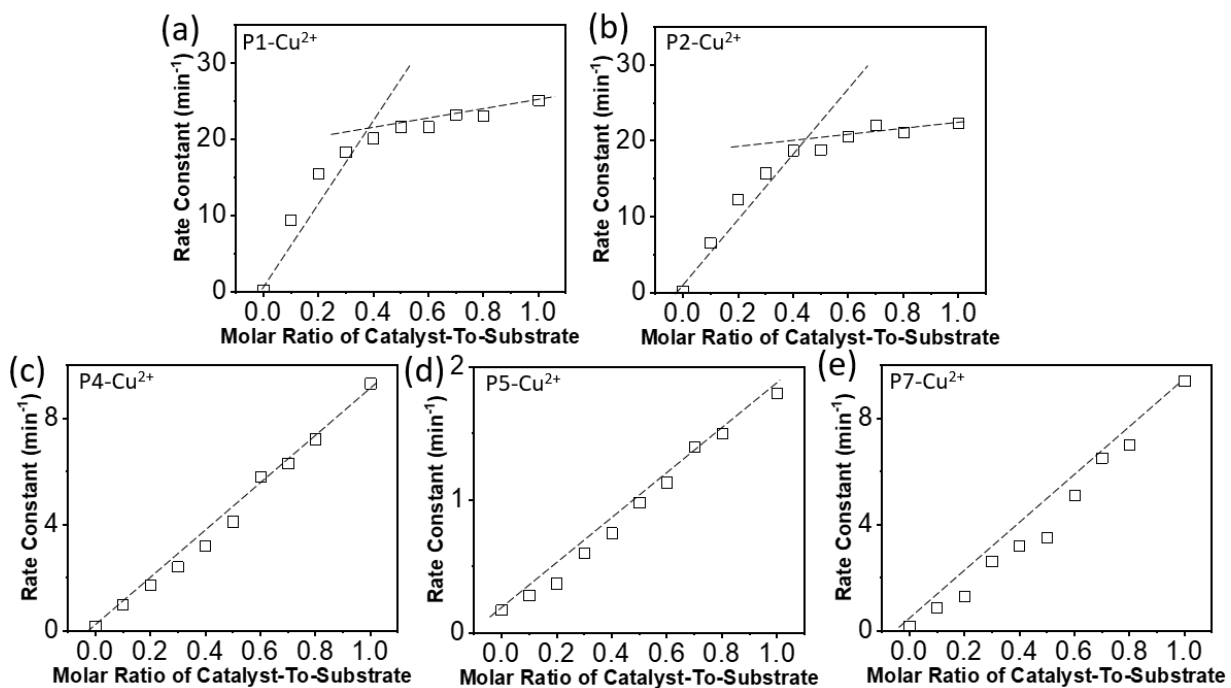


**Figure S9.** Saturation kinetics plots of PNPP hydrolysis catalyzed by (a) P1-Cu<sup>2+</sup> (b) P2-Cu<sup>2+</sup> (c) P4-Cu<sup>2+</sup> (d) P5-Cu<sup>2+</sup> and (e) P7-Cu<sup>2+</sup> respectively. Reaction conditions: [PNPP] = 27 μM; [Cu<sup>2+</sup>] = 1.4 to 24 μM; T = 25 °C. PBS buffer with pH = 7.0.

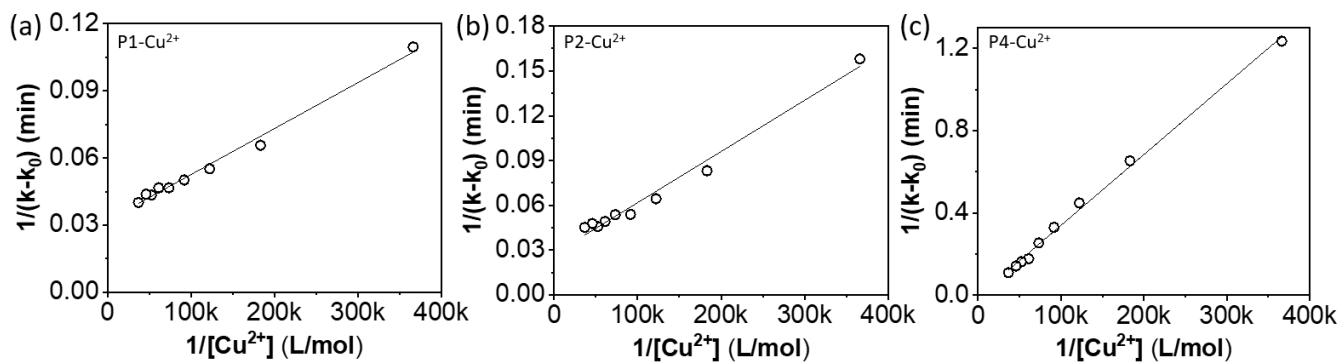


**Figure S10.** Saturation kinetics fitting plots of PNPP hydrolysis catalyzed by Cu<sup>2+</sup> containing micelle of (a) P1-Cu<sup>2+</sup> and (b) P2-Cu<sup>2+</sup> and (c) P4-Cu<sup>2+</sup>. Reaction conditions: [PNPP] = 27 μM; [Cu<sup>2+</sup>] = 1.4 to 27 μM; T = 25 °C. PBS buffer with pH = 7.0.

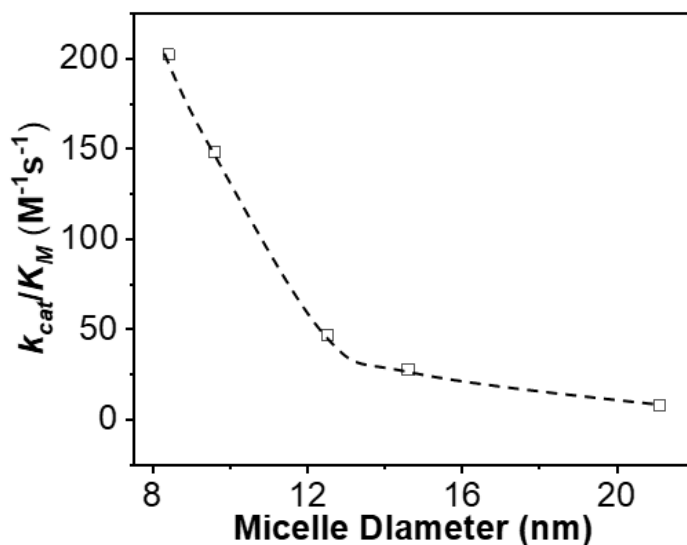


**Figure S11.**  $k_{cat}/K_M$  plotted as a function of the micellar diameter.

**Table S1.** The best fitted SAXS results of micelles from P1-Cu<sup>2+</sup>, P2-Cu<sup>2+</sup>, P4-Cu<sup>2+</sup>, P5-Cu<sup>2+</sup>, and P7-Cu<sup>2+</sup>.

Parameters	P1-Cu <sup>2+</sup>	P2-Cu <sup>2+</sup>	P4-Cu <sup>2+</sup>	P5-Cu <sup>2+</sup>	P7-Cu <sup>2+</sup>
Scale	0.007 (fixed)	0.000757 (fixed)	0.00987 (fixed)	0.01029 (fixed)	0.01040 (fixed)
Radius (Å)	42 ± 1	48 ± 1	73 ± 1	105 ± 1	65.8 ± 1
Shell thickness (Å)	-	-	47 ± 1	40 ± 1	53.9 ± 1
$\rho_{\text{core}}$ (10 <sup>-6</sup> Å <sup>-2</sup> )	-	-	9.74 ± 0.01	9.7 ± 0.004	9.48 (fixed)
$\rho_{\text{shell}}$ (10 <sup>-6</sup> Å <sup>-2</sup> )	-	-	8.19 (fixed)	8.19 (fixed)	8.0 ± 0.01

**Table S2.** The best fitted SAXS results of micelles from P3, P3-Cu<sup>2+</sup>, P6 and P6-Cu<sup>2+</sup>.

Parameters	P3	P3-Cu <sup>2+</sup>	P6	P6-Cu <sup>2+</sup>
Scale	0.013 (fixed)	0.00953 (fixed)	0.0094 (fixed)	0.01016 (fixed)
Radius (Å)	68.6 ± 1	62.3 ± 1	69.9 ± 1	69.9 ± 1
Shell thickness (Å)	39.7 ± 1	41.3 ± 1	42.2 ± 1	42.2 ± 1
$\rho_{\text{core}}$ (10 <sup>-6</sup> Å <sup>-2</sup> )	9.48 ± 0.006	9.62 ± 0.005	9.48 (fixed)	9.48 (fixed)
$\rho_{\text{shell}}$ (10 <sup>-6</sup> Å <sup>-2</sup> )	8.19 (fixed)	8.19 (fixed)	8.0 ± 0.01	8.0 ± 0.01

## References

1. Hasell, T.; Thurecht, K. J.; Jones, R. D.; Brown, P. D.; Howdle, S. M., Novel One Pot Synthesis of Silver Nanoparticle–Polymer Composites by Supercritical Co 2 Polymerisation in the Presence of a Raft Agent. *Chem. Comm* **2007**, 3933-3935.
2. Ording-Wenker, E. C.; Siegler, M. A.; Lutz, M.; Bouwman, E., Catalytic Catechol Oxidation by Copper Complexes: Development of a Structure–Activity Relationship. *Dalton Trans.* **2015**, *44*, 12196-12209.
3. Yang, L., Using an in-Vacuum Ccd Detector for Simultaneous Small-and Wide-Angle Scattering at Beamline X9. *Journal of synchrotron radiation* **2013**, *20*, 211-218.
4. Fan, L.; Degen, M.; Bendle, S.; Grupido, N.; Ilavsky, J. In *The Absolute Calibration of a Small-Angle Scattering Instrument with a Laboratory X-Ray Source*, Journal of Physics: Conference Series, IOP Publishing: 2010; p 012005.
5. Guinier, A.; Fournet, G.; Yudowitch, K. L., Small-Angle Scattering of X-Rays. **1955**.
6. Hayter, J. B.; Penfold, J., An Analytic Structure Factor for Macroion Solutions. *Molecular Physics* **1981**, *42*, 109-118.
7. Hansen, J.-P.; Hayter, J. B., A Rescaled Msa Structure Factor for Dilute Charged Colloidal Dispersions. *Molecular Physics* **1982**, *46*, 651-656.
8. Hammouda, B.; Kim, M.-H., The Empirical Core-Chain Model. *Journal of Molecular Liquids* **2017**, *247*, 434-440.
9. Hore, M. J.; Hammouda, B.; Li, Y.; Cheng, H., Co-Nonsolvency of Poly (N-Isopropylacrylamide) in Deuterated Water/Ethanol Mixtures. *Macromolecules* **2013**, *46*, 7894-7901.